doi:10.1016/j.jmb.2007.01.003 J. Mol. Biol. (2007) 367, 514–526

JMB

Available online at www.sciencedirect.com

ScienceDirect

ELSEVIER

Structural Basis of SspB-tail Recognition by the Zinc Binding Domain of ClpX

Eun Young Park[1], Byung-Gil Lee[1], Seung-Beom Hong[1] Hyung-Wook Kim[2], Hyesung Jeon[3] and Hyun Kyu Song[1]*

[1]*School of Life Sciences and Biotechnology Korea University Seoul 136-701, Korea*

[2]*Research Institute National Cancer Center Gyeonggi-Do 411-764, Korea*

[3]*Biomedical Research Center Korea Institute of Science and Technology, Seoul 136-791 Korea*

**Corresponding author*

The degradation of ssrA(AANDENYALAA)-tagged proteins in the bacterial cytosol is carried out by the ClpXP protease and is markedly stimulated by the SspB adaptor protein. It has previously been reported that the amino-terminal zinc-binding domain of ClpX (ZBD) is involved in complex formation with the SspB-tail (XB: ClpX-binding motif). In an effort to better understand the recognition of SspB by ClpX and the mechanism of delivery of ssrA-tagged substrates to ClpXP, we have determined the structures of ZBD alone at 1.5, 2.0, and 2.5 Å resolution in each different crystal form and also in complex with XB peptide at 1.6 Å resolution. The XB peptide forms an antiparallel β-sheet with two β-strands of ZBD, and the structure shows a 1:1 stoichiometric complex between ZBD and XB, suggesting that there are two independent SspB-tail-binding sites in ZBD. The high-resolution ZBD: XB complex structure, in combination with biochemical analyses, can account for key determinants in the recognition of the SspB-tail by ClpX and sheds light on the mechanism of delivery of target proteins to the prokaryotic degradation machine.

© 2007 Elsevier Ltd. All rights reserved.

Keywords: ATP-dependent protease; ClpXP; crystal; delivery complex; ssrA tag

Introduction

Energy-dependent proteases are involved in essential quality control tasks of cells under normal growth and stress conditions.[1,2] In eukaryotes, the ATP-dependent 26 S proteasome is a key player in the breakdown of intracellular proteins.[3,4] In prokaryotes, the biochemical and structural characteristics of a number of ATP-dependent proteases, including ClpXP, ClpAP, HslVU, Lon, and FtsH, have been studied.[1,5,6] Among these, ClpXP, ClpAP, and HslVU are two-component systems, consisting of a peptidase (ClpP and HslV) and an ATPase (ClpX, ClpA, and HslU). The proteolytic component must be tightly regulated by the ATPase component, otherwise they would act as a potentially dangerous degradation machine without clear substrate preference. These ATPases are members of the Hsp100 family,[7] possess unfoldase and/or chaperone activities,[8] and adopt typical hexameric ring-shaped structures.[9–12] Although they share significant sequence similarity at the core ATPase domain (AAA-ATPase domain), the extra domains that influence substrate recognition differ markedly.[13] HslU has a unique insertion domain (I-domain) in the middle of the structure, while ClpX and ClpA possess N-terminal domains, which also show different primary sequences.[10,14,15] ClpX and ClpA share a common protease, ClpP, but show different substrate preferences that might be derived from differences in the N-terminal substrate recognition domains of the ATPase components.

These domains play an essential role in the selection of target substrates. The N-terminal domain of ClpA has been shown to be important in substrate binding as well as in binding to ClpS cofactor.[16–18] The I-domain in HslU has been shown to be important in the degradation of SulA protein substrate, although no cofactor has yet been identified for HslU.[19] The N-terminal region of ClpX is known to be a C4-type zinc-binding domain (ZBD) and is also responsible for the recognition of

Abbreviations used: SspB-CHis, carboxy-terminal histidine tagged SspB protein; SspB-ClpX, SspB and ClpX fusion protein; SspB-ZBD, SspB and zinc binding domain of ClpX fusion protein; XB, ClpX-binding motif in SspB; ZBD, zinc binding domain of ClpX.

E-mail address of the corresponding author: hksong@korea.ac.kr

0022-2836/$ - see front matter © 2007 Elsevier Ltd. All rights reserved.

several target substrates including bacteriophage MuA:DNA transposase complexes, λO replication protein, and the UmuD′ subunit of error-prone DNA polymerase.[15,20,21] The ZBD of ClpX is a stable dimer in solution, while full-length ClpX is a hexameric ATPase, and thus has been proposed as a model consisting of a trimer-of-dimers.[22] The X-ray structure of the core ATPase domain from *Helicobacter pyroli* and the solution structure of the ZBD from *Esherichia coli* have been reported.[22,23] Interestingly, ClpXP-dependent degradation of a certain class of substrates such as ssrA-tagged proteins and RseA is greatly enhanced by the presence of an additional cofactor, SspB protein.[24–26]

This SspB adaptor molecule for ClpXP has received a great deal of attention recently,[24,26–31] and it has been reported that the C-terminal segment of SspB (XB: ClpX-binding region) and the ZBD of ClpX play a crucial role in tethering the delivery complex.[29,30] SspB was originally identified as a protein induced under starvation conditions[32] and was later found to bind specifically to ssrA-tagged substrates and enhance the recognition of these proteins by ClpX.[24] The structure of the SspB protein has been reported from two different sources, as well as in complex with ssrA peptide.[31,33] The SspB protein is a very stable dimer in solution, like the ZBD, and each ssrA-binding site of SspB is occupied in the complex structure.[31,33] Only the N-terminal two-thirds of the polypeptide chain of SspB protein is structurally ordered and contains the ssrA-binding site, while approximately 50 amino acid residues of the C-terminal region are known to be unstructured based on primary sequence analysis, circular dichroism, and limited proteolysis studies.[33] Only the very end of the C-terminal region shows significant sequence conservation among the several bacterial species, and this region has been shown to be important in interacting with ClpX.[29,30] Despite the vast range of experimental techniques that have been employed to investigate the mechanism of delivery of ssrA-tagged substrates to ClpX by SspB, including designed mutagenesis, fluorescence spectroscopy, and biochemical assays, little insight has been gained regarding details of the interaction due to a lack of structural information concerning the complex between ClpX and SspB.

In an effort to better understand the recognition of SspB by ClpX and the delivery mechanism of ssrA-tagged substrates to ClpXP ATP-dependent proteases, we have determined the crystal structure of the *E. coli* ZBD of ClpX alone at 1.5, 2.0, and 2.5 Å resolution in each different crystalline lattice and in complex with the XB peptide at 1.6 Å resolution. The ZBD structure shows a fold similar to that of the treble clef zinc-finger proteins.[22] The XB peptide forms an antiparallel β-sheet with two β-strands of the ZBD, and the structure shows that there are two independent XB-binding sites in ZBD. This contrasts with the reported stoichiometry of only one XB peptide per ZBD dimer obtained from biochemical techniques.[27] Further biochemical analyses of SspB-ClpX and SspB-ZBD fusion proteins shed light on the mechanisms of delivery of target proteins to the prokaryotic degradation machine.

Results

Structure determination

A truncated construct of SspB missing the 38 C-terminal amino acid residues (SspB127) showed no activation of ATPase activity of ClpX[33] and did not form a complex with the ZBD during gel filtration (Figure 1(a)). Two independent reports suggesting that the very end of the SspB tail is crucial for interaction with the ZBD were published previously.[29,30] Since crystallization of the complex between the ZBD and full-length SspB failed to yield crystals suitable for structure determination, we synthesized the XB peptide (NH_2-APALRVVK-COOH) according to the sequence information and previously determined biochemical data.[29,30] Crystallization trials with the ZBD alone yielded two different forms of crystal that diffracted X-rays to 2.0 and 1.5 Å resolution, and co-crystallization of the ZBD with XB peptide produced a complex crystal that diffracted to a resolution of 1.6 Å. The molecular replacement method was first tried using a solution structure of the ZBD (PDB ID: 1OVX), but this failed to yield acceptable results. Given that there are no methionine residues in the ZBD, we set out to mutate several residues with hydrophobic nature (Ile27, Ile28, and Cys43) to methionine. Selenomethionine-derivatized mutant proteins were not crystallized under the same conditions as the wild-type protein. However, a new hexagonal crystal form that possessed a monomeric ZBD in the asymmetric unit along with the C43M mutant was obtained under different crystallization conditions employed (see Materials and Methods). The selenomethionine-substituted C43M mutant structure was phased by multi-wavelength anomalous dispersion (MAD) methods (Table 1). The free ZBD structure determined at a resolution of 1.5 Å was used as a model for determination of the ZBD-XB complex structure by molecular replacement (see Materials and Methods). The refinement statistics for the model are shown in Table 1.

Overall structure

The structure shows a similar fold to that of the treble clef zinc-finger proteins.[22] The compact ZBD homodimer is formed by the tight interaction of each monomer, consisting of a β-hairpin capped at the C-terminal end by a long α-helix (Figure 2(b)). The longest ZBD model among four different structures spans residues Ser8–Leu51 (Figure 2(d)). The first seven residues (Thr1–Gly7) of the ZBD were not observed in terms of the electron density and are likely to be unstructured, and two C-terminal residues were observed in all different crystal forms. However, the chain directions differed. This most likely represents regional flexibility, and these

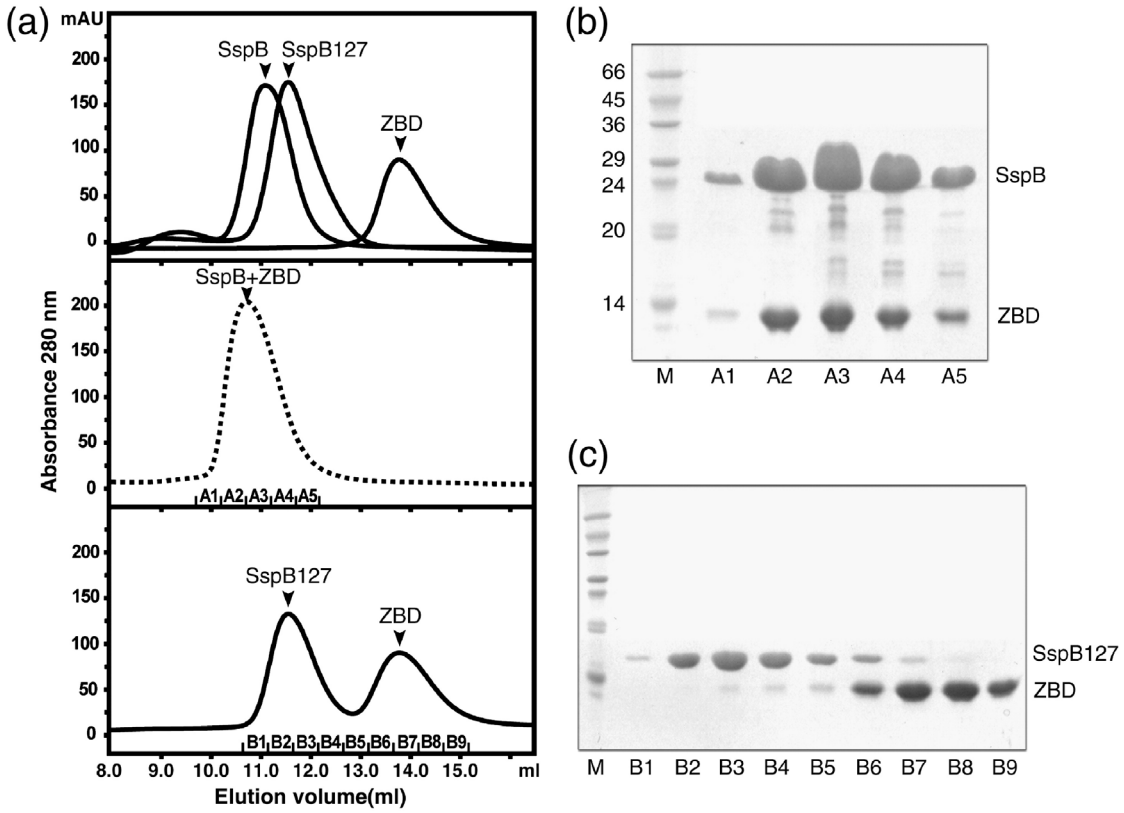

Figure 1. Biochemical analysis of the ZBD of ClpX. (a) Complex formation of the ZBD of ClpX and SspB protein determined by gel filtration chromatography. Top, elution profiles of individual proteins, full-length SspB, SspB127, and ZBD. Middle, SspB and ZBD mixture. Bottom, SspB127 and ZBD mixture. (b) Coomassie blue-stained, SDS-PAGE gel showing gel filtration results of the SspB:ZBD complex. Each lane corresponds to the fraction obtained from gel filtration using SspB and the ZBD mixture (middle in (a)). (c) Fractions from SspB127 and the ZBD mixture (bottom in (a)). The lane labeled as M represents molecular weight markers.

residues were not assigned in the solution structure.[22] A strong electron density for the zinc ion was observed without the addition of zinc ion under the crystallization conditions employed. Four sulfur atoms of conserved cysteine residues (Cys14, Cys17, Cys36, and Cys39) tetrahedrally coordinated to the zinc ion with average distances of between 2.34 and 2.39 Å, falling within the frequently observed range.[34] Interestingly, there is significant structural variation in the zinc-binding region when compared with the solution structure (Figure 2(d)).

The ZBD dimer forms a hydrophobic core comprising six residues from each chain.[22] The 19 Å long C-terminal α-helix (α1) in each molecule is also very important for dimerization. Indeed, a significant portion of the C43M mutant behaved as a monomer in solution when assessed by gel filtration analysis, and a monomer or distorted dimer in the hexagonal crystalline lattice was also observed (data not shown). Dimerization of the ZBD is crucial for interaction with the XB peptide (Figure 2(a)). The XB peptide binds to a hydrophobic groove formed by one region of the ZBD dimer and forms antiparallel β-sheets by main chain hydrogen-bonding with the first β-strand β1 (Figure 2(a)). The XB-binding groove is nearly perpendicular to the 2-fold symmetry axis of the ZBD dimer. Thus, the two XB peptides bound by the ZBD dimer are antiparallel to one another and run in the opposite direction from their N to C-terminals (Figure 2(a)). This symmetry suggests a general mode of association with the ClpX unfoldase. Dimeric ZBD shows distant similarity to a portion of the RING finger domain of Ubcm4-interacting protein 4 (PDB ID: 1WIM; Z-score = 2.9 from Dali Server) and the U-box domain of Prp19 (PDB ID: 1N87; Z-score = 2.7). However, it is unclear whether the observed structural similarity reflects any functional relationship. Nevertheless, it is interesting to note that these proteins act as a domain for the recognition of protein substrates.

SspB-tail recognition

Comparison of the free and complexed structures reveals little conformational change upon binding of the SspB C-terminal tail (Figure 2(d)). The root-mean-square deviation between free and XB-complexed states is 0.61 Å for all 41 C^{α} atoms (residues 10–50). The most significant rearrangements occur in the C-terminal region pointing to the ATPase domain of ClpX, which represents flexibility in this ZBD domain (Figure 2(d)). The direction of the polypeptide chain is opposite in the extreme case, and displacement of the position equivalent to the C^{α} atom (Glu50) is 6.7 Å. The ZBD:XB interaction buries a total of ~500 $Å^2$ of solvent-accessible

Table 1. Data collection and refinement statistics

	Orthorhombic	Tetragonal	Complex	Hexagonal (MAD)		
Data collection						
Space group	$P2_12_12_1$	$P4_12_12$	$P2_12_12_1$	$P6_422$		
Cell dimension						
a, *b*, *c* (Å)	32.5, 43.4, 67.7	42.6, 42.6, 128.3	32.6, 46.6, 57.0	41.1, 41.1, 102.2		
α, β, γ (°)	90, 90, 90	90, 90, 90	90, 90, 90	90, 90, 120		
				Remote	Edge	Peak
Wavelength (Å)	1.0	1.5418	1.0	0.95	0.97924	0.97868
Resolution (Å)[a]	1.5 (1.55)	2.0 (2.03)	1.6 (1.66)		2.5 (2.59)	
R_{sym} (%)[a,b]	6.7 (62.8)	4.5 (30.4)	5.9 (42.7)	5.1 (33.8)	5.1 (30.3)	6.0 (30.0)
$I/\sigma(I)$	22.2 (1.4)	37.4 (9.2)	27.7 (1.9)	71.7 (7.2)	71.2 (7.1)	71.0 (7.0)
Total reflections	55,194	33,762	53,936	42,262	42,009	41,872
Unique reflections	13,866	7652	11,450	2074	2074	2073
Completeness (%)[a]	86.8 (45.9)	89.3 (93.5)	94.5 (64.1)	99.6 (98.0)	99.6 (98.0)	99.5 (99.5)
FOM before/after DM[c]					0.571/0.641 (2.5 Å)	
Refinement						
Resolution range (Å)	50–1.5	50–2.0	50–1.6	30–2.5		
Number of reflections	13,235	7550	10,887	2009		
R_{work}/R_{free} (%)[d]	18.5/22.1	26.5/31.2	20.2/22.5	23.9/27.2		
Number of atoms						
Protein	675	651	745	291		
Water	125	74	86	7		
Zn^{2+}/Ca^{2+}/PEG400	2/1/13	2/0/0	2/0/0	1/0/0		
r.m.s deviations						
Bond length (Å)	0.0087	0.0047	0.0035	0.0056		
Bond angles (°)	1.323	1.198	1.088	1.103		
Average *B*-value (Å^2)						
Main/side-chain	12.9/16.2	27.5/31.7	20.6/24.2	53.3/56.3		
Water	31.3	40.1	37.9	57.5		
Zn^{2+}/Ca^{2+}/PEG400	10.3/21.2/48.9	28.5/–/–	14.8/–/–	49.1/–/–		
Ramachandran outliers	None	None	None	None		

[a] Values in parentheses are for reflections in the highest resolution bin.
[b] $R_{merge} = \sum_h \sum_i | I(h,i) - \langle I(h) \rangle | / \sum_h \sum_i I(h,i)$, where $I(h,i)$ is the intensity of the *i*th measurement of *h* and $\langle I(h) \rangle$ is the corresponding average value for all *i* measurements.
[c] Figure of merit $= | \sum P(\alpha) e^{i\alpha} / \sum P(\alpha) |$, where $P(\alpha)$ is the phase probability distribution and α is the phase.
[d] R_{work} and $R_{free} = \sum || F_O | - | F_C || / \sum | F_O |$ for the working set and test set (10%) of reflections.

surface†. Additional interactions are presented in Figure 3. In our complexed structure, the XB peptide binds in a β-strand conformation to a groove formed by the β1 strand and the α1 helix (Figure 2(a)). We were able to build the last six residues (ALRVVK) of the eight residue XB peptide (Figure 3(b)). Five of these six residues appear to form the key region in determining the specificity of the interactions with ZBD. The N-terminal region of the XB backbone beyond Leu161(p) extends away from the ZBD ((p) is used to designate the residue in the SspB peptide). XB binding is stabilized by numerous hydrophobic and hydrogen bond interactions involving both the peptide backbone and side-chains (Figure 3(a)). Extensive mutational studies show that hydrophobic Leu161(p) is a key determinant in the interaction with the ZBD, as this side-chain extends into the hydrophobic pocket formed by Phe16(A), Leu42(A), and Ile46(A) of the ZBD ((A) and (B) are used to designate these residues in the different chains of the ZBD).[29,30] Arg162(p) in the peptide is not conserved; however, main chain atoms of that residue make critical hydrogen bond interactions with the backbone amide and carbonyl groups of Ala29(B). The hydrophobic side-chain of Val163(p) interacts with the side-chain of Ile46(A), and the bifurcated side-chain atoms of Val164(p) interact with Leu12(B) and Ala29(B). The last residue Lys165(p) seems to interact with several ZBD residues. An epsilon nitrogen atom in the side-chain hydrogen bonds with backbone oxygen atoms of Gln21(B) and Val24(B). Interestingly, the terminal carboxylate group forms a hydrogen bond with the backbone amide of Leu27(B) and a possible ionic interaction with the side-chain nitrogen atom of Lys26(B). However, this ionic interaction does not seem to be crucial since SspB-CHis (SspB with eight extra residues at the C terminus; ELHHHHHH) stimulates proteolytic activity of the ClpXP complex in a manner similar to that of SspB (Figure 4(d)). Furthermore, the mutant with deletion of the last Lys165(p) residue of SspB possesses almost the same activity as the wild-type protein.[30]

Activity of SspB-ClpX fusion protein

In an effort to delineate the substrate delivery mechanism, we generated an SspB-ClpX chimeric variant (a designed adaptor:AAA-ATPase fusion protein) based on the obtained structural information. The N-terminal region of the ZBD (Thr1–Gly7) is invisible in the electron density map, which reflects

† http://www.biochem.ucl.ac.uk/bsm/PP/server/

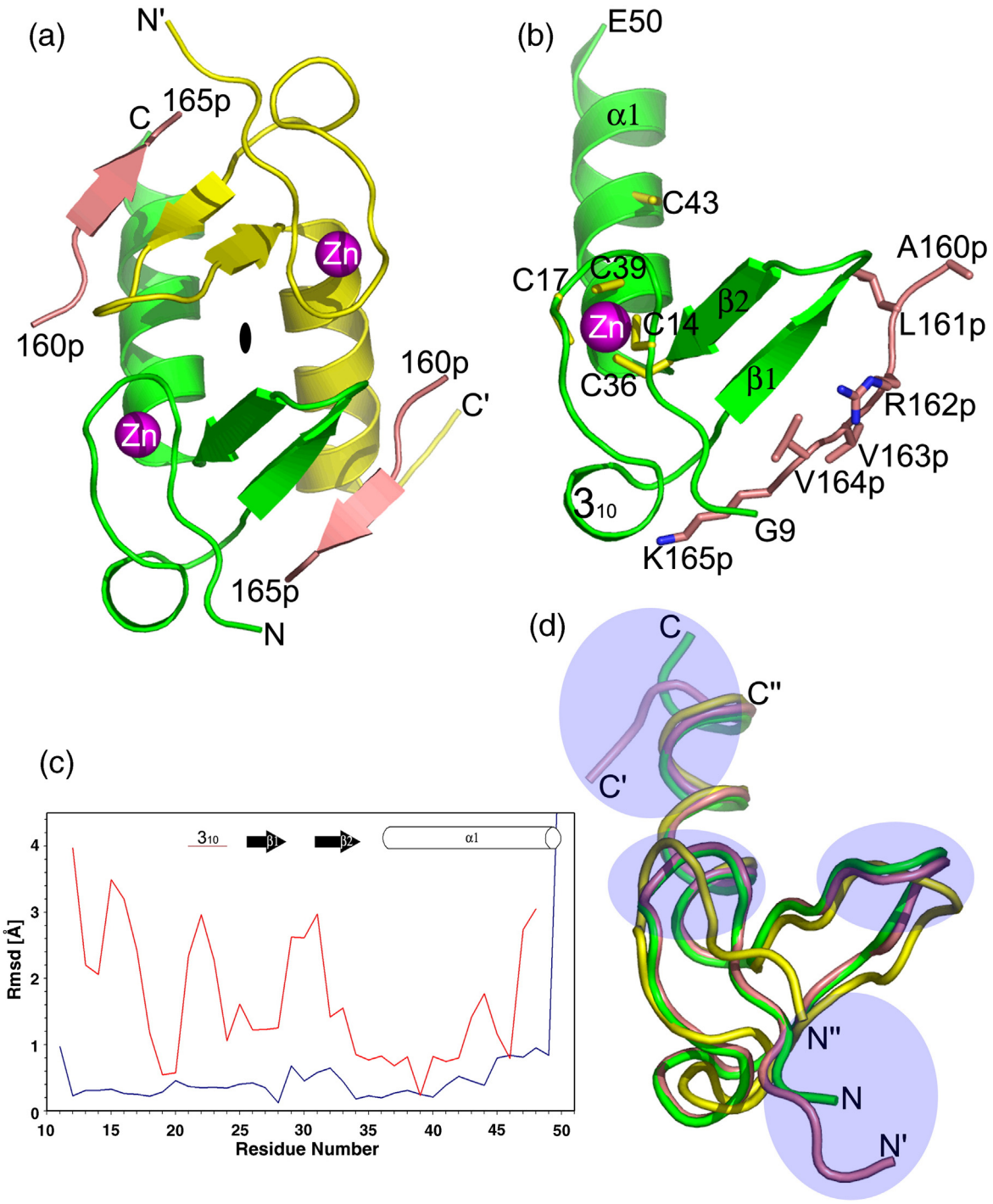

Figure 2. Structure of the ZBD-XB complex. (a) Ribbon diagram showing the dimeric ZBD-XB complex structure viewed along the non-crystallographic 2-fold molecular symmetry axis. Each monomer in the ZBD is colored green and yellow. The bound XB peptide and zinc ion are colored salmon and purple, respectively. The N and C termini of the ZBD are labeled, as are the first and last residues of the XB peptide (160p and 165p). (b) Ribbon diagram showing the monomer of the ZBD and details of bound XB peptide. The view is almost the same as in (a). Side-chains of five cysteine in the ZBD and XB peptide are shown, and secondary structural elements of the ZBD and the residues drawn are labeled. (c) Plot of the difference between free and complexed ZBD models. The RMS differences for the main chain atoms of each residue are plotted as a function of residue number (free ZBD *versus* XB-ZBD complex, blue line; free ZBD *versus* ZBD NMR structure, red line). The secondary structural elements are indicated. (d) Backbone superposition of free (green), free NMR (yellow), and the XB complex (salmon) structure. N and C termini of the ZBD and the regions showing significant structural movement are marked with transparent ovals.

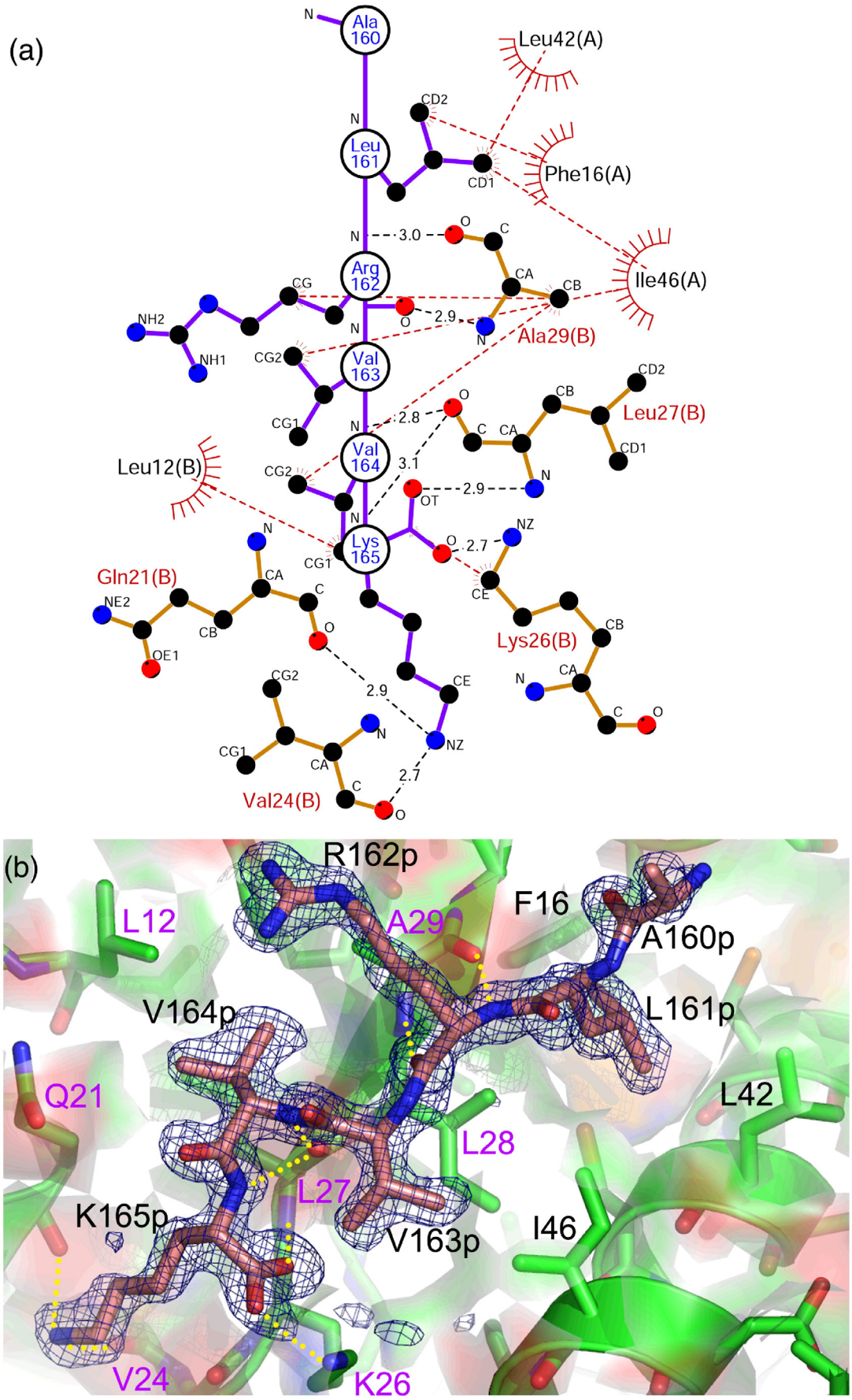

Figure 3 (*legend on next page*)

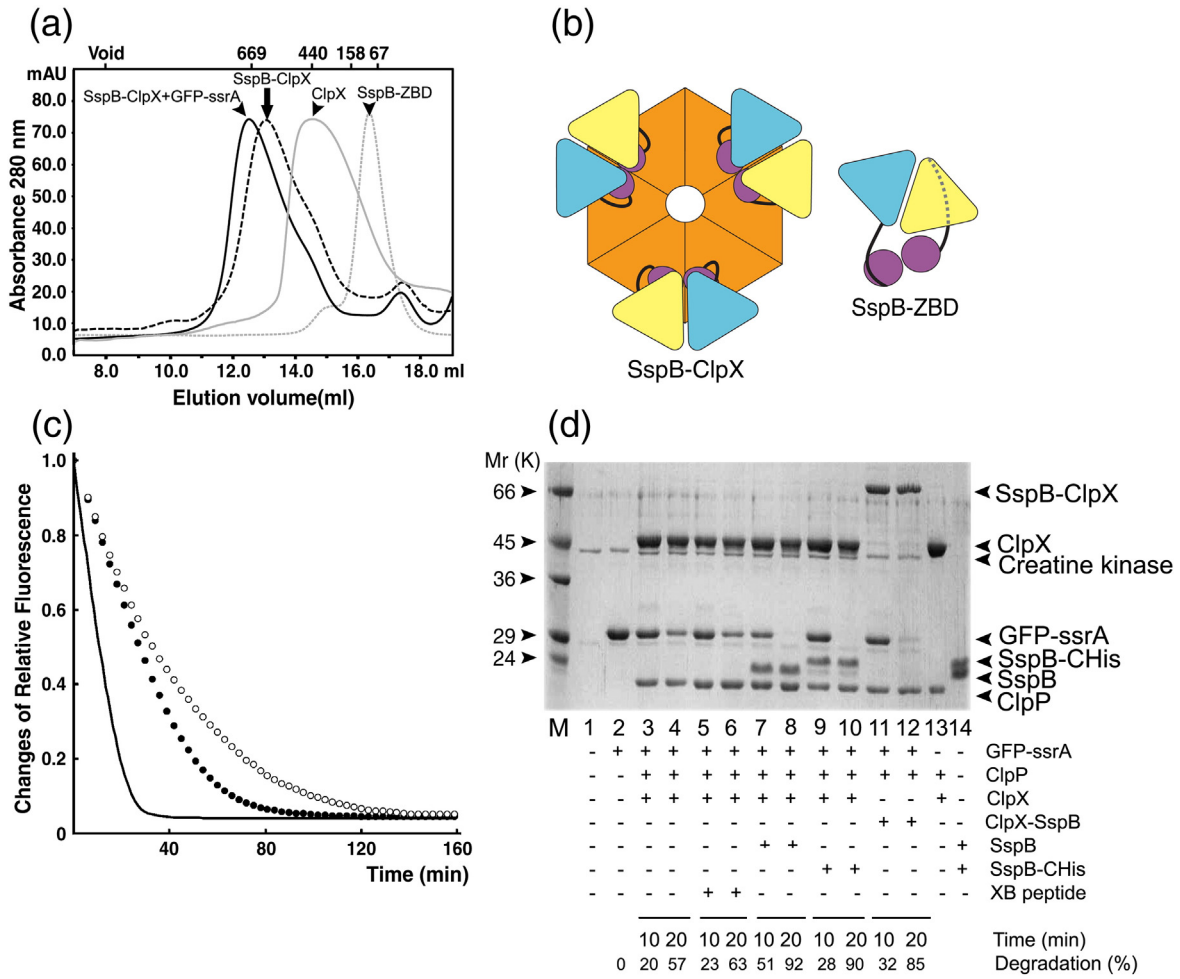

Figure 4. Biochemical characterization of the SspB-ClpX fusion protein. (a) Gel filtration profile of SspB-ClpX fusion protein alone (broken line) and in complex with GFP-ssrA (continuous line). Gel filtration profile of ClpX (continuous line in grey) and SspB-ZBD fusion protein (broken line in grey) were appended for comparison. (b) Schematic models of SspB-ClpX and SspB-ZBD fusion protein (see the text for details). Dimeric SspB protein is colored yellow and cyan, dimeric ZBD is colored purple, and hexameric AAA-ATPase domain of ClpX is colored orange. (c) Degradation of substrate GFP-ssrA was monitored with fluorescent technique. Continuous line is ClpXP degradation activity in the presence of SspB. Filled circle is SspB-ClpX and ClpP degradation activity and open circle is clpXP degradation without SspB. (d) Degradation of substrate GFP-ssrA by ClpXP was monitored with various combinations of adaptors (none, XB peptide, SspB, SspB-CHis, covalent attachment of SspB to ClpX) with an ATP regeneration system (in the presence of creatine kinase and creatine phosphate). Note that XB peptide does not enhance the proteolytic activity of ClpXP (lanes 3–6), whereas SspB, SspB-CHis, and covalent linkage of SspB showed similar proteolytic activity (lanes 7–12).

its high flexibility, and the distance between the last residue of XB (165(p)) and the first modeled residue of ZBD is relatively short (approximately 12.5 Å). Therefore, it seemed feasible to generate an SspB-ClpX fusion protein without marked structural distortion. Firstly, enhancement of the proteolytic activity of the ClpXP complex was monitored in the presence of SspB-CHis in order to determine whether additional residues at the C terminus may affect the function of SspB directly. A comparison of the proteolytic activity of ClpXP with GFP-ssrA substrate in the presence of either SspB or SspB-CHis (Figure 4(d), lanes 7–10) suggested that there was no effect following the attachment of extra residues to the C terminus of SspB. Secondly, a smaller chimeric protein, SspB-ZBD, was generated to examine the solubility and proper assembly of the SspB-ZBD dimer (Figure 4(a)). The gel filtration profile of SspB-ZBD showed that SspB and the ZBD dimer form independently with the extra two-residue linker inserted into the region between SspB and the ZBD (Figure 4(a)). Finally, SspB-ClpX fusion protein was

Figure 3. XB peptide-binding site of the ZBD. (a) Schematic diagram showing interactions between the ZBD and XB peptide. Hydrophobic interactions are denoted by red starbursts and broken lines; hydrogen-bonding interactions by black broken lines. This panel was drawn using LIGPLOT.[52] (b) A view of the electron density map showing the bound XB peptide and its binding site in the ZBD. The $|F_o–F_c|$ map (dark grey color) was calculated prior to inclusion of the illustrated XB peptide residues in the model. This map was calculated using 30–1.6 Å data and is contoured at 2.7 σ. This panel was drawn using PyMOL [http://pymol.sourceforge.net/].

generated and the proper assembly of three dimeric SspB and hexameric ClpX was confirmed by the gel filtration elution profile (Figure 4(a)). Furthermore, the SspB-ClpX fusion protein was able to form a stable complex with the GFP-ssrA substrate (Figure 4(a)). With this intriguing chimeric protein, we have confirmed the proteolytic activity against GFP-ssrA in the presence of stoichiometric amounts of ClpP (Figure 4(c), lanes 11 and 12 and (d)). The SspB-ClpX chimera:ClpP complex shows almost similar activity to the SspB:ClpX:ClpP ternary delivery complex, suggesting that two tails of dimeric SspB may interact with each binding dimeric ZBD (see Discussion for details).

Discussion

Sequence recognition by the ZBD

Mass spectroscopic analysis of trapped substrates of the *E. coli* proteome using a tagged and inactive variant of ClpP revealed at least five classes of ClpX-recognizing motifs: two located at the C terminus (C-motif 1: LAA-COOH, ssrA-type; C-motif 2: RRKKAI-COOH, MuA-type) and three at the N terminus (N-motif 1: polar-T/ϕ-ϕ-basic-ϕ; N-motif 2: NH_2-Met-basic-ϕ-ϕ-ϕ; N-motif 3: ϕ-x-polar-x-polar-x-basic-polar).[35] Recognition of these signals for protein degradation by ClpXP is tightly regulated by additional factors. For example, denaturation of substrates during heat-shock or following proteolytic cleavage of substrates exposes latent ClpX-recognition sequences, and adaptor molecules are needed for efficient delivery of substrates in some cases.[25,36,37] SspB enhances the delivery of RseA and ssrA-marked protein substrates (C-motif 1) to ClpXP.[24,25] RssB targets σ^S (N-motif 1) to ClpXP,[38,39] and UmuD confers instability on UmuD′ (the recognition motif remains unclear).[21] Similar sequence motifs (156-GGRPAL*RVV*K-165 in SspB; 327-GGRLRL*MLS*AE-337 in RssB; 9LREI-12 in UmuD) in these adaptor molecules are known to be essential for interaction with ClpX *via* the ZBD.[29,30,36] Dougan and colleagues analyzed the sequence motif that interacts with the ZDB of ClpX, and a consensus sequence, GG(R/K)xxLx(V/L), has been proposed.[29] The sequence of UmuD is not aligned with that of SspB and RssB, but in all three cases, the critical residue is leucine (boldface above sequence). Our crystal structure showed that the upper conserved sequence GG(R/K) in SspB and RssB does not contribute to the affinity between the adaptor molecule and the ZBD (Figures 2(a) and 3(a)). It is reasonable to assume that the LREI residues of UmuD share the same binding site of the ZBD with SspB and RssB. Our high-resolution complexed structure revealed that Leu161(p) is a key determinant (Figure 3(a)) and is consistent with the extensive mutational data with SspB protein[29,30] and the critical role of Leu9 in UmuD.[36] Therefore, the hydrophobic side-chain of Leu332 in RssB and Leu9 in UmuD might interact with the side-chains of Phe16, Leu42, and Ile46 in the ZBD, as does the side-chain of Leu161(p) in SspB (Figure 3), although the importance of Leu332 (and of Leu334) in RssB remains to be confirmed by biochemical and mutational experiments. The other interactions are basically main chain–main chain interactions that act to form an antiparallel β-sheet and additional hydrophobic contacts (Figure 3). Although delineation of the consensus sequence is difficult to derive from the minimal sequence-specific interaction, the main feature of this binding motif for the ZBD represents fully exposed hydrophobic residues. Both structures of full-length SspB and active UmuD′ show that the C-terminal region in SspB and the N-terminal region in UmuD form an additional structural unit separated by a core domain structure and are fully exposed to the solvent.[31,33,40] Although structural details are not available, the secondary structure of the region interacting with ZBD in SspB, RssB, and UmuD is predicted‡ (data not shown) to consist of a β-strand shown in the current ZBD:XB complex structure (Figure 2(a)). In contrast to SspB and UmuD, RssB does not possess a long random coil region in the protein and, thus, conserved glycine residues (Gly325, Gly327, and Gly328) might be important because they confer flexibility on the C-terminal tail of RssB to facilitate delivery of substrate σ^S to the ClpXP complex.

Implications for the mechanism of substrate delivery

There are several proposed mechanisms of the delivery of substrate by SspB.[27,29,33] A possible mode of association in which the 2-fold axis of SspB is aligned with the 6-fold axis of ClpX and a mechanism in which the orientation of the SspB dimer is such that the C terminus of the ssrA-tag extends toward ClpX have both been proposed given the observed dimer:hexamer stoichiometry of the SspB:ClpX interaction.[33,41] However, it would be expected that the aligned symmetry would be broken when the substrates are delivered into one hexameric ClpX pore and, moreover, there is a fundamental flaw in that the SspB interacting layer in ClpX is a trimer-of-dimers (or at least a pseudo-trimer), and therefore, complex formation between the SspB dimer and ZBD trimer does not sustain the aligned symmetry. Dougan and colleagues suggested that complete restoration of the SspB:ClpXP system can already be achieved when only one SspB-binding site is present within the ClpX . Therefore, a complex committed to substrate translocation and degradation only requires the docking of a single SspB dimer to one site within the ClpX hexamer and not the simultaneous interaction of an SspB dimer with two ClpX subunits within the hexamer.[29] Later, Baker and Sauer used an elegant protein-design study to show that both tails of SspB with their XB modules are required for efficient delivery.[27] Based on their

‡ http://bioinf.cs.ucl.ac.uk/psipred/

biochemical data, the ClpX hexamer contains three XB-binding sites, one per ZBD dimer, and thus binds strongly to just one SspB dimer at a time.

However, the structural data that we have revealed here contrast a previous report[27] because each SspB-tail-binding site in the ZBD is equally occupied by two XB peptides (Figures 2(a) and 3(b)). Therefore, there are a total of six independent tethering sites in hexameric ClpX. In the previous model, it was determined that once a dynamic single tail of SspB bound to an XB-binding site in the ZBD, the other tail subsequently interacted with the unoccupied tethering site in the neighboring ZBD dimer. The soluble and active SspB-ClpX fusion protein could not be generated in that manner because the six linked tails between core SspB and ZBD have to be entangled. Therefore, the molecular arrangement of SspB to the ClpX hexamer should occur in sequence in our functional SspB-ClpX fusion protein. The sequential arrangement may entail one tail in the SspB dimer interacting with a ZBD, after which the other tail interacts with the closest XB-binding site in the neighboring ZBD. We speculate that this arrangement is unfavorable because the molecular weight of SspB-ZBD fusion protein determined by gel filtration chromatography represents its molecular architecture shown in Figure 4(b). Taken together with the solution behavior of chimeric proteins and high resolution complex structure, we suggest the molecular arrangement of SspB-ClpX fusion protein that is shown as Figure 4(b). It is worthwhile to note that the 1:1 binding stoichiometry between SspB dimer and ClpX hexamer is generally accepted in the field,[41] but our SspB-ClpX fusion complex differs. From our observations, the delivery complex (SspB: ClpXP) is quite labile, and no stable complex could be detected using biochemical techniques including gel filtration and isothermal titration calorimetry (data not shown). Although it is not directly related, many prokaryotic ATP-dependent proteases such as HslVU, ClpXP, and ClpAP could not be used to form stable complexes and exist as different stoichometric complexes.[19,42–44] Therefore, the existence of the 3:1 stoichiometry of SspB:ClpX, which is shown in our SspB-ClpX fusion protein, should be confirmed further by other techniques. Regardless of the binding stoichiometry, based on the current structural and biochemical data, we could suggest that one of the three ZBD dimers is sufficient to generate a delivery complex with SspB, and considering the known 1:1 binding stoichiometry between SspB and ClpX, we were able to deduce that the functional unit can be the ZBD dimer.[41] Given the current experimental data presented here, we cannot completely rule out the model proposed by Bolon *et al.*[27] Instead, we suggest another plausible model for the substrate delivery by SspB protein to the ClpXP protease (Figure 5).

Recently, large nucleotide-dependent movement of the ZBD has been reported.[45] The ZBDs are proposed to switch from a captured state in which the ZBDs are distal from ClpP and are located on the top of the hexameric ring of AAA-ATPase domain to a feeding state in which at least one ZBD dimer moves into the AAA-ATPase ring and becomes proximal to ClpP.[45] If this information is combined with the model proposed by Bolon *et al.*,[27] at least two separate ZBD dimers might undergo the large conformational change simultaneously. However, our current model showing that a SspB dimer bound to a ZBD dimer works together to feed ssrA-tagged substrate might be much simpler and energetically favorable (Figure 5).

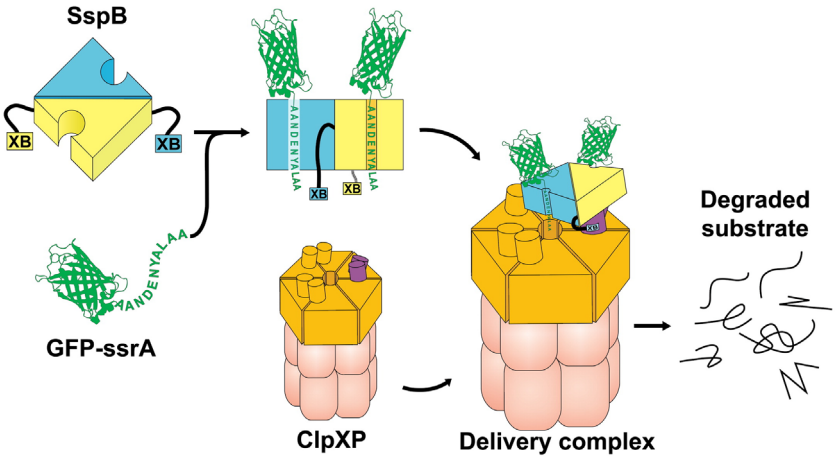

Figure 5. A proposed model for substrate delivery by SspB protein to the ClpXP protease. An ssrA-tagged target protein (GFP-ssrA) was synthesized by bacterial ribosomes. SspB protein recognized the N-terminal 2/3 (AANDENY) of the 11 amino acid residues of the ssrA tag and delivered the substrate to ClpXP. One hexameric ClpX was removed in the ClpXP complex for simplicity. At this stage, SspB associated with the ZBD at the top of ClpXP using two C-terminal tails (XB). The ZBD is a trimer-of-dimers, and two tails of SspB might interact with two independent binding sites in the ZBD dimer, as shown in Figure 4(b). Following this interaction, the substrate docks onto the main body of ClpX and the ATPase domain of ClpX recognizes the LAA motif at the very end of the ssrA tag. The recognized substrate is fully unfolded by ClpX in an ATP-dependent manner and translocated into the proteolytic chamber of the ClpP protease.

In summary, we have presented here the molecular details regarding the formation of the complex between ClpX and SspB protein. Furthermore, bivalent tethering of dimeric SspB to dimeric ZBD generates a functional complex for efficient substrate delivery. However, it remains to be determined whether bivalent tethering of a dimeric SspB to two separate ZBD dimers in full-length ClpX can yield a functional complex. Ultimately, the unambiguous determination of a model of the delivery complex will require structural analysis of a complex between full-length SspB and ClpX.

Materials and Methods

Sample preparation

E. coli ClpX, ClpP, SspB, SspB-CHis, and GFP-ssrA were prepared by the same procedure as described.[33] The N-terminal fragment 1–63 of ClpX was cloned using standard polymerase chain reaction (PCR) techniques. The cloned fragments were flanked by NdeI and BamHI restriction enzyme sites, and the fragments were ligated into pET-15b expression vectors. The integrity of the resultant plasmids was verified by DNA sequencing. Given the failure in obtaining a crystal that diffracted well using a longer construct, a shorter construct of the ZBD was generated by insertion of a termination codon after Leu51 using the QuikChange method. The plasmids were then transformed into BL21(DE3) cells. Expression of the ZBD was induced by the addition of 1 mM IPTG at $A_{600\ nm}=0.6$ in the presence of 0.1 mM zinc chloride. The cells were centrifuged and kept frozen at −80 °C until further use. The cell pellet was resuspended in ice-cold 50 mM Tris-HCl (pH 8.0) containing 100 mM NaCl and subsequently disrupted by ultrasonication. The proteins were applied to a Ni-NTA column in the first step. Eluents from the column were analyzed by SDS-PAGE and visualized by Coomassie blue staining. Fractions containing the ZBD were pooled and thrombin (1:1000 molar ratio) was added. The target protein (with histidine tag removed) was loaded onto a Hi-Trap Q-Sepharose anion exchange column and further purified by gel filtration using Superose 12 pre-equilibrated with 20 mM Hepes-NaOH (pH 7.5) containing 100 mM NaCl. Given that there no methionine residues are present in the ZBD, several different residues (Ile27, Ile28, and Cys43) were replaced by Met using the QuikChange method to introduce the possibility of selenomethinine derivatization. Selenomethionyl-ZBD mutants were expressed in B834(DE3) cells and purified in a similar manner as the wild-type protein. Electron spray ionization mass spectroscopic (ESI-MS) analysis was carried out to confirm the incorporation of selenomethionine in the purified protein samples. Synthesized XB peptides (XB: APALRVVK) were purchased from Anygen Co., Ltd.

SspB-ClpX and SspB-ZBD fusion proteins

The full-length SspB gene was cloned into pET-22b vector with NdeI and XhoI restriction enzyme sites, while the ClpX and ZBD genes were cloned separately into pET-15b with NdeI and BamHI. For construction of SspB-ClpX and SspB-ZBD fusion protein, PCR-based site-directed mutagenesis (QuikChange) of the full-length SspB construct was carried out to cause a change in sequence from XhoI (CTCGAG) to NdeI (CATATG). The plasmids were cut with NdeI restriction enzyme, treated with CIAP (Calf Intestinal Alkaline Phosphatase), and then ligated into pET-15b vector containing the ClpX or ZBD gene. As a result, a fusion construct was composed of an N-terminal histidine tag, full-length SspB, and ClpX or ZBD. Cells were grown to mid-log phase at 37 °C in LB medium, and protein expression was induced by the addition of 1 mM IPTG. Following incubation for 22 h at 22 °C for SspB-ClpX and incubation for 5 h at 37 °C for SspB-ZBD, cells were harvested by centrifugation and frozen at −20 °C until further use. The purification procedure employed for these chimeric proteins was similar to that of ClpX or the ZBD alone.

Biochemical assays

Proteins were quantified by their absorbance at 280 nm or by the Bradford method. Degradation of GFP-ssrA by ClpXP was performed at 37 °C in 50 mM Hepes-KOH (pH 7.5), 80 mM KCl, 10 mM MgCl, 10% (v/v) glycerol, 0.02% NP-40, 1 mM DTT with an ATP regeneration system (5 mM ATP, 8 mM creatine phosphate, 50 μg/ml creatine kinase). ClpX and ClpP were used at concentrations of 360 and 300 nM, respectively. ClpXP was pre-incubated for 2 min at 30 °C with all assay components except substrate GFP-ssrA protein (3.7 μM). Following proteolysis, the activity was visualized by SDS-PAGE and Coomassie blue staining. The activity was quantified by digitally scanning the gel and then determining the band intensity using AlphaEase®FC software for Windows (Alpha Innotech Corp.).

For monitoring of the fluorescence decrease of GFP-ssrA, a similar assay condition was applied with 0.3 μM ClpX, 0.9 μM ClpP, 2 μM GFP-ssrA, 0.9 μM SspB and 0.3 μM SspB-ClpX fusion protein. Assay buffer contains 25 mM Hepes-KOH (pH 7.6), 5 mM KCl, 5 mM $MgCl_2$, 10% glycerol, and 0.032% NP40 in the presence of ATP regeneration system (0.32 mg/ml creatine kinase, 16 mM creatin phosphate, 5 mM ATP). Degradation activity was measured by spectrofluorometer (RF5301PC, Shimadzu, Japan) at room temperature (excitation, 467 nm; emission, 511 nm).

Complex formation in solution was confirmed by gel filtration chromatography using Superose 6 or 12 columns attached to an FPLC system. The column was pre-equilibrated with 50 mM Tris-HCl (pH 8.0), 150 mM NaCl, 1 mM DTT. The absorbance was monitored at 280 nm.

Crystallization and data collection

The purified ZBD was concentrated to 17 mg/ml in 50 mM Tris-HCl (pH 7.7), 100 mM NaCl, 2 mM β-mercaptoethanol. Crystallization was performed by the hanging-drop vapor diffusion method conducted at 22 °C, and three different crystal forms of free ZBD were obtained. The reservoir solution for the tetragonal crystal consisted of 100 mM tri-sodium citrate (pH 5.6), 2% (v/v) ethyleneimine polymer, and 500 mM NaCl. Diffraction data were collected on an imaging plate using laboratory X-rays. The reservoir solution for the orthorhombic form consisted of 100 mM Hepes-NaOH (pH 7.5), 200 mM calcium chloride, and 27–30% (v/v) polyethylene glycol 400. For cryo-cooling, a crystal was transferred to a reservoir solution containing 5% glycerol before flash-freezing in a nitrogen stream at 100 K. Using seleno-

methionine-derivatized C43M mutant, the two previously mentioned crystal forms were not reproduced. Instead, a new hexagonal crystal form was obtained under crystallization conditions utilizing 100 mM sodium acetate (pH 4.6), 200 mM lithium sulfate, and 8–12% (v/v) 2-propanol. MAD data were collected on a CCD detector at the 4A beamline of Pohang Accelerator Laboratory, Pohang, Republic of Korea.

For ZBD:XB complex crystallization, a tenfold molar excess of solid XB peptide was added and the mixture was incubated for 30 min at 4 °C. The complex was crystallized for ten days over a reservoir of 1.6 M tri-sodium citrate (pH 6.5). For cryo-cooling, the crystal was transferred to 1.25 M tri-sodium citrate, 90 mM Hepes-KOH (pH 7.5) containing 10% glycerol before flash-freezing in a nitrogen stream at 100 K. The highest resolution native diffraction data using orthorhombic crystals of free ZBD and ZBD-XB complex were collected on a CCD detector at the NW12 beamline of Photon Factory, Tsukuba, Japan. The diffraction data were processed and scaled using the HKL2000 software package.[46] Statistics for the collected data are described in Table 1.

Structure determination and refinement

One possible selenium site in the asymmetric unit of the hexagonal crystal form was located using SOLVE and the phases were improved with RESOLVE.[47] Statistics for the phasing are shown in Table 1. The electron density was of sufficient quality to identify and build a long C-terminal α-helix and a zinc-binding site. Initially, the ZBD coordinates determined by NMR (PDB ID: 1OVX) were superimposed onto the α-helix manually, and the model was then rebuilt using the O program.[48] The protein model was refined with CNS.[49] Solvent molecules were added using model-phased difference Fourier maps.[49]

Phases of the other crystal forms were obtained by molecular replacement with the PHASER program[50] using refined monomeric ZBD as a search model. Refinement of the models was performed as described above. The 2-fold non-crystallographic symmetry was maintained with tight restraint during the early stages of refinement, but was relaxed in the final rounds. Phases of the complex crystal were also obtained by molecular replacement with the PHASER program[50] using a refined 1.5 Å resolution model of dimeric ZBD as a search model. The positions of the XB peptide were clearly determined using a model-phased difference Fourier map contoured at 3.0 σ. Refinement of the models was also performed as described above. Six out of eight residues in the XB peptide were built and no electron density was observed for the N-terminal alanine and proline residues. Statistics for the refined structures are also shown in Table 1. The assessment of model geometry and the assignment of secondary structure elements were performed using the PROCHECK program.[51]

Protein Data Bank accession codes

The coordinates have been deposited in the RCSB Protein Data Bank with the accession codes codes 2DS5 (orthorhombic), 2DS6 (tetragonal), 2DS7 (hexagonal) for free ZBD, and 2DS8 for the ZBD-XB complex.

An NMR titration with SspB peptide and biochemical study on the zinc binding domain of ClpX were reported recently.[53] The interacting residues are consistent with our data in general, but a suggested model for the interaction between SspB dimer and ClpX hexamer is different from our interpretation.

Acknowledgements

We thank the staff at 4A beamline, Pohang Accelerator Laboratory, Republic of Korea and NW12 beamline, Photon Factory, Japan for help with data collection. We also thank Drs P. Zwickl (Max-Planck-Institute for Biochemistry, Germany) and T. Tamura (National Institute of Advanced Industrial Science and Technology, Japan) for cells containing His-GFP-ssrA and Professor M. J. Eck for his generous support during the initial stage of this project. This work was supported by the Korea Research Foundation Grant (KRF-2006-312-C00249) funded by the Korean Government (MOEHRD) and by the Korea Science and Engineering Foundation Grant (KOSEF, R01-2004-000-10773-0) funded by the Korea government (MOST). E.Y.P. was supported by a Seoul Science Fellowship.

References

1. Gottesman, S. (1996). Proteases and their targets in *Escherichia coli*. *Annu. Rev. Genet.* **30**, 465–506.
2. Wickner, S., Maurizi, M. R. & Gottesman, S. (1999). Posttranslational quality control: folding, refolding, and degrading proteins. *Science*, **286**, 1888–1893.
3. Goldberg, A. L. (2003). Protein degradation and protection against misfolded or damaged proteins. *Nature*, **426**, 895–899.
4. Pines, J. & Lindon, C. (2005). Proteolysis: anytime, any place, anywhere? *Nature Cell Biol.* **7**, 731–735.
5. Sauer, R. T., Bolon, D. N., Burton, B. M., Burton, R. E., Flynn, J. M., Grant, R. A. *et al.* (2004). Sculpting the proteome with AAA(+) proteases and disassembly machines. *Cell*, **119**, 9–18.
6. Bochtler, M., Ditzel, L., Groll, M., Hartmann, C. & Huber, R. (1999). The proteasome. *Annu. Rev. Biophys. Biomol. Struct.* **28**, 295–317.
7. Neuwald, A. F., Aravind, L., Spouge, J. L. & Koonin, E. V. (1999). AAA+: a class of chaperone-like ATPases associated with the assembly, operation, and disassembly of protein complexes. *Genome Res.* **9**, 27–43.
8. Seong, I. S., Oh, J. Y., Lee, J. W., Tanaka, K. & Chung, C. H. (2000). The HslU ATPase acts as a molecular chaperone in prevention of aggregation of SulA, an inhibitor of cell division in *Escherichia coli*. *FEBS Letters*, **477**, 224–229.
9. Hanson, P. I. & Whiteheart, S. W. (2005). AAA+ proteins: have engine, will work. *Nature Rev. Mol. Cell. Biol.* **6**, 519–529.
10. Bochtler, M., Hartmann, C., Song, H. K., Bourenkov, G. P., Bartunik, H. D. & Huber, R. (2000). The structures of HsIU and the ATP-dependent protease HsIU-HsIV. *Nature*, **403**, 800–805.
11. Beuron, F., Maurizi, M. R., Belnap, D. M., Kocsis, E., Booy, F. P., Kessel, M. & Steven, A. C. (1998). At sixes and sevens: characterization of the symmetry mismatch of the ClpAP chaperone-assisted protease. *J. Struct. Biol.* **123**, 248–259.
12. Kessel, M., Wu, W., Gottesman, S., Kocsis, E., Steven, A. C. & Maurizi, M. R. (1996). Six-fold rotational symmetry of ClpQ, the E. coli homolog of the 20S proteasome, and its ATP-dependent activator, ClpY. *FEBS Letters*, **398**, 274–278.
13. Mogk, A., Dougan, D., Weibezahn, J., Schlieker, C., Turgay, K. & Bukau, B. (2004). Broad yet high

substrate specificity: the challenge of AAA+ proteins. *J. Struct. Biol.* **146**, 90–98.
14. Lo, J. H., Baker, T. A. & Sauer, R. T. (2001). Characterization of the N-terminal repeat domain of *Escherichia coli* ClpA-A class I Clp/HSP100 ATPase. *Protein Sci.* **10**, 551–559.
15. Banecki, B., Wawrzynow, A., Puzewicz, J., Georgopoulos, C. & Zylicz, M. (2001). Structure-function analysis of the zinc-binding region of the ClpX molecular chaperone. *J. Biol. Chem.* **276**, 18843–18848.
16. Dougan, D. A., Reid, B. G., Horwich, A. L. & Bukau, B. (2002). ClpS, a substrate modulator of the ClpAP machine. *Mol. Cell*, **9**, 673–683.
17. Guo, F., Esser, L., Singh, S. K., Maurizi, M. R. & Xia, D. (2002). Crystal structure of the heterodimeric complex of the adaptor, ClpS, with the N-domain of the AAA+ chaperone, ClpA. *J. Biol. Chem.* **277**, 46753–46762.
18. Singh, S. K., Rozycki, J., Ortega, J., Ishikawa, T., Lo, J., Steven, A. C. & Maurizi, M. R. (2001). Functional domains of the ClpA and ClpX molecular chaperones identified by limited proteolysis and deletion analysis. *J. Biol. Chem.* **276**, 29420–29429.
19. Song, H. K., Hartmann, C., Ramachandran, R., Bochtler, M., Behrendt, R., Moroder, L. & Huber, R. (2000). Mutational studies on HslU and its docking mode with HslV. *Proc. Natl Acad. Sci. USA*, **97**, 14103–14108.
20. Levchenko, I., Luo, L. & Baker, T. A. (1995). Disassembly of the Mu transposase tetramer by the ClpX chaperone. *Genes Dev.* **9**, 2399–2408.
21. Frank, E. G., Ennis, D. G., Gonzalez, M., Levine, A. S. & Woodgate, R. (1996). Regulation of SOS mutagenesis by proteolysis. *Proc. Natl Acad. Sci. USA*, **93**, 10291–10296.
22. Donaldson, L. W., Wojtyra, U. & Houry, W. A. (2003). Solution structure of the dimeric zinc binding domain of the chaperone ClpX. *J. Biol. Chem.* **278**, 48991–48996.
23. Kim, D. Y. & Kim, K. K. (2003). Crystal structure of ClpX molecular chaperone from *Helicobacter pylori*. *J. Biol. Chem.* **278**, 50664–50670.
24. Levchenko, I., Seidel, M., Sauer, R. T. & Baker, T. A. (2000). A specificity-enhancing factor for the ClpXP degradation machine. *Science*, **289**, 2354–2356.
25. Flynn, J. M., Levchenko, I., Sauer, R. T. & Baker, T. A. (2004). Modulating substrate choice: the SspB adaptor delivers a regulator of the extracytoplasmic-stress response to the AAA+ protease ClpXP for degradation. *Genes Dev.* **18**, 2292–2301.
26. Levchenko, I., Grant, R. A., Flynn, J. M., Sauer, R. T. & Baker, T. A. (2005). Versatile modes of peptide recognition by the AAA+ adaptor protein SspB. *Nature Struct. Mol. Biol.* **12**, 520–525.
27. Bolon, D. N., Wah, D. A., Hersch, G. L., Baker, T. A. & Sauer, R. T. (2004). Bivalent tethering of SspB to ClpXP is required for efficient substrate delivery: a protein-design study. *Mol. Cell*, **13**, 443–449.
28. Bolon, D. N., Grant, R. A., Baker, T. A. & Sauer, R. T. (2004). Nucleotide-dependent substrate handoff from the SspB adaptor to the AAA+ ClpXP protease. *Mol. Cell*, **16**, 343–350.
29. Dougan, D. A., Weber-Ban, E. & Bukau, B. (2003). Targeted delivery of an ssrA-tagged substrate by the adaptor protein SspB to its cognate AAA+ protein ClpX. *Mol. Cell*, **12**, 373–380.
30. Wah, D. A., Levchenko, I., Rieckhof, G. E., Bolon, D. N., Baker, T. A. & Sauer, R. T. (2003). Flexible linkers leash the substrate binding domain of SspB to a peptide module that stabilizes delivery complexes with the AAA+ ClpXP protease. *Mol. Cell*, **12**, 355–363.
31. Levchenko, I., Grant, R. A., Wah, D. A., Sauer, R. T. & Baker, T. A. (2003). Structure of a delivery protein for an AAA+ protease in complex with a peptide degradation tag. *Mol. Cell*, **12**, 365–372.
32. Williams, M. D., Ouyang, T. X. & Flickinger, M. C. (1994). Starvation-induced expression of SspA and SspB: the effects of a null mutation in sspA on *Escherichia coli* protein synthesis and survival during growth and prolonged starvation. *Mol. Microbiol.* **11**, 1029–1043.
33. Song, H. K. & Eck, M. J. (2003). Structural basis of degradation signal recognition by SspB, a specificity-enhancing factor for the ClpXP proteolytic machine. *Mol. Cell*, **12**, 75–86.
34. Harding, M. M. (2006). Small revisions to predicted distances around metal sites in proteins. *Acta Crystallog. sect. D*, **62**, 678–682.
35. Flynn, J. M., Neher, S. B., Kim, Y. I., Sauer, R. T. & Baker, T. A. (2003). Proteomic discovery of cellular substrates of the ClpXP protease reveals five classes of ClpX-recognition signals. *Mol. Cell*, **11**, 671–683.
36. Neher, S. B., Sauer, R. T. & Baker, T. A. (2003). Distinct peptide signals in the UmuD and UmuD′ subunits of UmuD/D′ mediate tethering and substrate processing by the ClpXP protease. *Proc. Natl Acad. Sci. USA*, **100**, 13219–13224.
37. Neher, S. B., Flynn, J. M., Sauer, R. T. & Baker, T. A. (2003). Latent ClpX-recognition signals ensure LexA destruction after DNA damage. *Genes Dev.* **17**, 1084–1089.
38. Becker, G., Klauck, E. & Hengge-Aronis, R. (1999). Regulation of RpoS proteolysis in *Escherichia coli*: the response regulator RssB is a recognition factor that interacts with the turnover element in RpoS. *Proc. Natl Acad. Sci. USA*, **96**, 6439–6444.
39. Zhou, Y., Gottesman, S., Hoskins, J. R., Maurizi, M. R. & Wickner, S. (2001). The RssB response regulator directly targets sigma(S) for degradation by ClpXP. *Genes Dev.* **15**, 627–637.
40. Peat, T. S., Frank, E. G., McDonald, J. P., Levine, A. S., Woodgate, R. & Hendrickson, W. A. (1996). Structure of the UmuD′ protein and its regulation in response to DNA damage. *Nature*, **380**, 727–730.
41. Wah, D. A., Levchenko, I., Baker, T. A. & Sauer, R. T. (2002). Characterization of a specificity factor for an AAA+ ATPase: assembly of SspB dimers with ssrA-tagged proteins and the ClpX hexamer. *Chem. Biol.* **9**, 1237–1245.
42. Wang, J., Song, J. J., Franklin, M. C., Kamtekar, S., Im, Y. J., Rho, S. H. *et al.* (2001). Crystal structures of the HslVU peptidase-ATPase complex reveal an ATP-dependent proteolysis mechanism. *Structure*, **9**, 177–184.
43. Ortega, J., Lee, H. S., Maurizi, M. R. & Steven, A. C. (2002). Alternating translocation of protein substrates from both ends of ClpXP protease. *EMBO J.* **21**, 4938–4949.
44. Ortega, J., Lee, H. S., Maurizi, M. R. & Steven, A. C. (2004). ClpA and ClpX ATPases bind simultaneously to opposite ends of ClpP peptidase to form active hybrid complexes. *J. Struct. Biol.* **146**, 217–226.
45. Thibault, G., Tsitrin, Y., Davidson, T., Gribun, A. & Houry, W. A. (2006). Large nucleotide-dependent movement of the N-terminal domain of the ClpX chaperone. *EMBO J.* **25**, 3367–3376.
46. Otwinowski, Z. & Minor, W. (1997). Processing of X-ray diffraction data collected in oscillation mode. *Methods Enzymol.* **276**, 307–326.

47. Terwilliger, T. C. (2003). Automated main-chain model building by template matching and iterative fragment extension. *Acta Crystallog. sect. D*, **59**, 38–44.
48. Jones, T. A., Zou, J.-Y., Cowan, S. W. & Kjeldgaard, M. (1991). Improved methods for binding protein models in electron density maps and the location of errors in these models. *Acta Crystallog. sect. A*, **47**, 110–119.
49. Brunger, A. T., Adams, P. D., Clore, G. M., DeLano, W. L., Gros, P., Grosse-Kunstleve, R. W. *et al.* (1998). Crystallography and NMR system: a new software suite for macromolecular structure determination. *Acta Crystallog. sect. D*, **54**, 905–921.
50. Vagin, A. & Teplyakov, A. (2000). An approach to multi-copy search in molecular replacement. *Acta Crystallog. sect. D*, **56**, 1622–1624.
51. Laskowski, R., MacArthur, M., Hutchinson, E. & Thorton, J. (1993). PROCHECK: a program to check the stereochemical quality of protein structures. *J. Appl. Crystallog.* **26**, 283–291.
52. Wallace, A. C., Laskowski, R. A. & Thornton, J. M. (1995). LIGPLOT: a program to generate schematic diagrams of protein-ligand interactions. *Protein Eng.* **8**, 127–134.
53. Thibault, G., Yudin, J., Wong, P., Tsitrin, V., Sprangers, R., Zhao, R. *et al.* (2006). Specificity in substrate and cofactor recognition by the N-terminal domain of the chaperone ClpX. *Proc. Natl. Acad. Sci. USA*, **103**, 17724–17729.

Edited by R. Huber

(Received 20 December 2006; accepted 2 January 2007)
Available online 9 January 2007